

# A hidden link in the LMC star cluster formation history

Andrés E. Piatti<sup>1,2\*</sup>

<sup>1</sup>*Instituto Interdisciplinario de Ciencias Básicas (ICB), CONICET-UNCuyo, Padre J. Contreras 1300, M5502JMA, Mendoza, Argentina*

<sup>2</sup>*Consejo Nacional de Investigaciones Científicas y Técnicas, Godoy Cruz 2290, C1425FQB, Buenos Aires, Argentina*

Accepted XXX. Received YYY; in original form ZZZ

## ABSTRACT

The age distribution function of star clusters in the Large Magellanic Cloud (LMC) is known to present a feature called the cluster age gap, a period of time from  $\sim 4$  to 11 Gyr ago with a remarkable small number of clusters identified. In this work we performed an in-depth analysis of three recently catalogued age gap cluster candidates with the aim of confirming their physical nature. We used GEMINI@GMOS  $g, i$  photometry centred on the objects to build colour-magnitude diagrams from which we recognised their main features. We also performed an automatic search of stellar over-densities using Gaussian mixture model techniques and analysed the corresponding colour-magnitude diagrams similarly as performed for the aforementioned candidates. The present GEMINI data sets would seem to discard any strong evidence of these object being real clusters, and rather support the possibility of the result of stellar density variations of the LMC field star distribution. These three objects, in addition to other 17 new identified candidates, are placed in the LMC outermost disc in a limited region toward the southwest from the LMC centre. They had embraced the possibility to answer the long-time conundrum about the absence of LMC age gap clusters. From an statistical approach, combined with the knowledge of the expected LMC age-metallicity relationship, and recent simulations of the interaction between the LMC and the Milky Way, we provide not only evidence against the physical nature of the studied objects, but also an interpretation on the lack of identification of more LMC age gap clusters.

**Key words:** technique:photometric – galaxies: individual: LMC – galaxies: star clusters

## 1 INTRODUCTION

The absence of star clusters -groups of tens to thousand stars with a common origin in space and time- with ages between  $\sim 4$  and 11 Gyr in the neighbouring galaxy, the Large Magellanic Cloud (LMC), is an astrophysical living enigma. The LMC has more than 3740 star clusters spanning its whole lifetime; 15 of them older than 11 Gyr (Bica et al. 2008; Piatti et al. 2019b), while hundreds of millions of field stars formed during that period (Harris & Zaritsky 2009). If the LMC had formed star clusters as it formed field stars during this age gap, nearly 20 star clusters would have been found (Massana et al. 2022). At present, three star clusters have been confirmed as LMC age gap clusters, namely: ESO 121-SC03 (Mateo et al. 1986), KMHK 1592 (Piatti 2022a), and KMHK 1762 (Gatto et al. 2022). Consequently, the absence of LMC age gap star clusters could imply a particular galaxy star formation history, which strikes our

understanding about galaxy formation and evolution processes.

Recently, Gatto et al. (2020) discovered 20 new age gap star cluster candidates based on ages estimated from colour-magnitude diagrams. This result sharply contrasts with those of different observational campaigns that have searched during the last decades for new LMC age gap clusters unsuccessfully (Da Costa 1991; Geisler et al. 1997). They also contrast with the effort of estimating ages for the vast majority of the catalogued LMC clusters, using recent or ongoing 4m-class telescope/satellite imaging surveys throughout the LMC, e.g., SMASH (Nidever et al. 2017), STEP (Ripepi et al. 2014), YMCA (Gatto et al. 2024), VMC (Cioni et al. 2011), *Gaia* DR3 (Gaia Collaboration et al. 2016; Babusiaux et al. 2023), etc. The resulting ages turned out to be younger than those of LMC age gap star clusters (Piatti et al. 2014; Piatti 2021a; Narloch et al. 2022). If more LMC age gap star clusters really exist, the above mentioned surveys fail to detect them because of their relatively shallow photometry do not undoubtedly reach the age gap star cluster main sequences in the colour-magnitude dia-

\* E-mail: andres.piatti@fcen.uncu.edu.ar

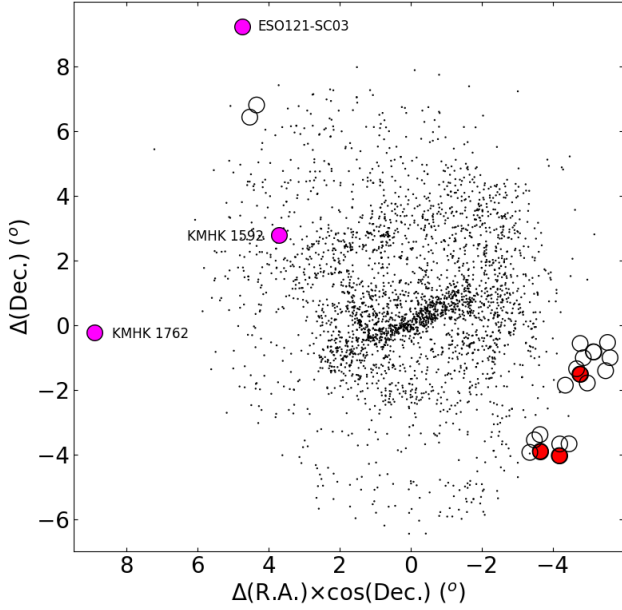


**Figure 1.** Spatial distribution of LMC star clusters (dots; [Bica et al. 2008](#)) and that of the objects studied in this work (red filled circles). Open and magenta filled circles represent others [Gatto et al. \(2020\)](#)'s LMC age gap candidates and confirmed LMC age gap clusters, respectively.

gram, which is mandatory to estimate star cluster ages. The second serious constraint is the very small number in [Gatto et al. \(2020\)](#)'s candidates ( $8 \pm 2$  versus more than 100 stars observed in real LMC age gap clusters; [Mateo et al. \(1986\)](#); [Piatti \(2022a\)](#)), that could indistinguishably be the result of a composite population of LMC field stars. Confirmed LMC age gap clusters should clearly show their main sequence turnoffs placed at magnitudes compatibles with the clusters' age and distance. The third constraint is the odd spatial distribution of [Gatto et al. \(2020\)](#)'s candidates, with clusters sharply concentrated in two areas and not distributed throughout the LMC. Figure 1 illustrates the spatial distribution of the population of LMC star clusters taken from the catalogue of [Bica et al. \(2008\)](#). The three confirmed LMC age gap star clusters and the new 20 ones are highlighted with large magenta and open circles, respectively. These constraints point to the need of 8m-class telescopes and high-spatial resolution imaging instruments in order to obtain much deeper and accurate star cluster colour-magnitude diagrams, and hence to obtain reliable clusters' ages to confirm genuine LMC age gap clusters.

There are very few theoretical speculations proposed to explain the existence of the LMC cluster age gap ([Bekki et al. 2004](#)), and still prevails a general lack of consensus in the community about its origin ([Gatto et al. 2022](#)). The available theoretical models on the formation and evolution of the LMC are based on a simple closed system with continuous star formation under the assumption of chemical homogeneity ([Da Costa & Hatzidimitriou 1998](#)), and on a bursting formation mechanism with an important formation event centred at  $\sim 2.0$  Gyr ([Pagel & Tautvaisiene 1998](#)). The models do not predict the interruption of cluster formation

during the gap age range, so that if clusters formed alongside the continuous field star formation, either in a closed box or bursting system, they should be discovered.

From recent time, the orbital motion of the LMC has been simulated with the aim of uncovering its past interaction history ([Besla et al. 2007](#); [Choi et al. 2022](#); [Schmidt et al. 2022](#); [Jiménez-Arranz et al. 2023](#)). Although these are timely efforts, the modelling of the orbital motions of its star cluster population in the context of the interaction with the Small Magellanic Cloud (SMC) and/or the Milky Way is still lacking. For instance, ([Carpintero et al. 2013](#)) simulated the orbital motions of SMC star clusters with the aim of exploring whether the lack of SMC star clusters older than  $\sim 7$  Gyr could be the result of the capture of them by the LMC. Indeed, they found that star clusters with orbital eccentricities larger than 0.4, which represent nearly 15% of the SMC clusters, are captured by the LMC. Another 20-50% of the SMC clusters are ejected into the intergalactic medium. Similarly, some LMC clusters could have been stripped off the main LMC body. An example of such a possible scenario is illustrated by a new LMC star cluster identified by [Piatti \(2016\)](#), which possibly reached its present position in the outer LMC disc after being scattered from the innermost LMC disc where it might have been born ([Piatti et al. 2019a](#)).

The absence or the small number of age gap clusters in comparison with the  $\sim 20$  expected ones will imply necessarily to consider improvements in the current LMC formation models. Assuming that the LMC should harbour  $\sim 20$  age gap clusters, the confirmation of any fraction of [Gatto et al. \(2020\)](#)'s objects as such will definitely lead to recover a comprehensive picture of the LMC formation history and to improve the models of the LMC formation and evolution, including scenarios of tidal interaction with neighbouring galaxies through unexplored channels; not coupled formation of clusters and field stars, etc. The larger the number of confirmed age gap clusters, the more the reliability of current theoretical models of the LMC formation and evolution. The less the number of confirmed age gap clusters, the more the possibility of improvements in the LMC formation models, if they are indeed confirmed as clusters instead of LMC composite field star populations. It is therefore necessary to definitively perform a robust statistics on the number of LMC age gap clusters. This is essential in order to suggest ways of improvement to the current LMC formation models.

Precisely, we embarked in an observational campaign aiming at confirming the real physical nature of these objects, and in the case of those confirmed as genuine star clusters to estimate their fundamental parameters. The resulting ages will be used to assess whether they are in the LMC age gap. In this work, we report results of three [Gatto et al. \(2020\)](#)'s objects that comprise all the observational material that we gathered from this campaign. Although they represent, quantitatively speaking, a relative small percentage of the new LMC age gap star cluster candidates, the confirmation of these objects as age gap star clusters, or a percentage of them, or even only one of them, has the potential to advance our understanding of the formation and evolution of the LMC and its dynamical interaction with other galaxies, among others. In Section 2 we describe the collected data and different procedures used to obtain the colour-magnitude diagrams. Section 3 deals with the analy-

sis of the colour-magnitude diagrams from the employment of different cleaning and clustering tools, while in Section 4 we discuss on the physical nature of the studied objects Section 5 summarizes the main conclusions of this work.

## 2 OBSERVATIONAL DATA

From the sample of 20 new LMC age gap star cluster candidates (Figure 1), STEP0004, STEP0012, and YMCA0012 were randomly selected by the GEMINI Observatory staff to be observed in queue mode at the GEMINI South telescope with the GMOS-S instrument (3×1 mosaic of Hamamatsu CCDs; 5.5×5.5 square arcmin FOV) through *g* and *i* filters under program GS-2024B-Q-214 (PI: Piatti). We obtained between 5 and 8 images per filter and per object in nights with excellent seeing (0.56'' to 0.97'' FWHM) and photometric conditions at a mean airmass of 1.5. We used individual exposure times of 200 sec and 79 sec for *g* and *i* filters, respectively, to prevent saturation. We reduced the data following the recipes documented at the GEMINI Observatory webpage<sup>1</sup> and employed the GEMINI@GMOS package in GEMINI@IRAF. We applied overscan, trimming, bias subtraction, flattening and mosaicing on all data images, with previously obtained nightly master calibration images (bias and flats). Then, we combined (added) all the programme images for the same object and filter with the aim of gaining in the reachable limiting magnitude. We found that the photometry depth increased nearly one mag with respect to the photometry depth reached by single programme images.

We used routines in the DAOPHOT/ALLSTAR suite of programs (Stetson et al. 1990) to find stellar sources and to fit their brightness profiles with point-spread-functions (PSFs) in order to obtain the stellar photometry of each summed image. For each of them, we obtained a preliminary PSF derived from the brightest, least contaminated  $\sim 40$  stars, which in turn was used to derive a quadratically varying PSF by fitting a larger sample of  $\sim 100$  star. Both groups of PSF stars were interactively selected. Then we used the ALLSTAR programme to apply the resulting PSF to the identified stellar objects. ALLSTAR generates a subtracted image which was used to find and measure magnitudes of additional fainter stars. We repeated this procedure three times for each summed image. Then, we combined all the independent *g*, *i* instrumental magnitudes using the stand-alone DAOMATCH and DAOMASTER programs<sup>2</sup>. As a result, we produced one data set per object containing the *x* and *y* coordinates of each star, the instrumental *g* and *i* magnitudes with their respective errors,  $\chi$ , and sharpness. Sharpness and  $\chi$  are image diagnostic parameters used by DAOPHOT. With the aim of removing bad pixels, unresolved double stars, cosmic rays, and background galaxies from the photometric catalogues, we kept sources with  $|\text{sharpness}| < 0.5$ .

Figure 2 shows the resulting photometry for the entire GMOS FOV; the studied objects covering a relatively small central circular area of radius 0.20-0.40 arcmin (Gatto et al. 2020). In order to build the colour-magnitude diagrams of Figure 2, we used the instrumental *g* magnitudes and *g* – *i*

colours shifted according to the necessary zero point offsets, which include the effect of interstellar reddening across the FOV ( $E(B - V)^3 = 0.055 \pm 0.005$  mag), to match the zero-age main sequence and the red giant clump of theoretical isochrones (Bressan et al. 2012, PARSEC version 2.1S<sup>4</sup>) corresponding to 4, 7, and 10 Gyr, respectively, which span the age range of the LMC age gap. Note that these offsets do not affect the assessment of the physical reality of the studied objects, nor the estimation of ages of genuine star clusters either. We also adopted a mean LMC distance modulus of  $(m - M)_o = 18.49$  mag (de Grijs et al. 2014), and an overall metallicity of  $[\text{Fe}/\text{H}] = -0.7$  dex, which is the mean metallicity value of the LMC age-metallicity relationship during the age gap period (Piatti & Geisler 2013). As can be seen, the colour-magnitude diagrams resulted to be more than 2 mag deeper than those obtained by Gatto et al. (2020). They would seem to reveal the presence of field star populations composed of intermediate-age ones (1-2 Gyr) to moderately old stars ( $\sim 10$  Gyr).

## 3 DATA ANALYSIS

### 3.1 Intrinsic colour-magnitude diagrams

The presence of a star cluster in a star field implies the existence of a local stellar overdensity with distinctive magnitude and colour distributions, whose stars delineate the cluster sequences in the colour-magnitude diagram. Hence, the colour-magnitude diagram observed along the cluster's line-of-sight contains information of both cluster and field stars. This means that if the colour-magnitude diagram features of the star field were subtracted, the intrinsic characteristics of the cluster colour-magnitude diagram would be uncovered. One possibility of carrying out such a distinction consists in comparing a star field colour-magnitude diagram with that observed along the cluster's line of sight and then to properly eliminate from the later a number of stars equal to that found in the former, bearing in mind that the magnitudes and colours of the eliminated stars in the cluster's colour-magnitude diagram must reproduce the respective magnitude and colour distributions in the star field colour-magnitude diagram. The resulting subtracted field star colour-magnitude diagram should depict the intrinsic features of that cleaned particular field that, in the case of being a star cluster, are the well known cluster's sequences.

We used a circular region around the centers of the studied objects with a radius equals to twice their radii, which were estimated from previously constructed stellar radial profiles based on star counts. We adopted for the three objects a radius of 0.40 arcmin, in very good agreement with the radii quoted in Table B1 of Gatto et al. (2020). Similarly, we devised 1000 star field circles with the same radius of the objects' circles and centred at four times the objects' radii. They were randomly distributed around the objects' circles. We then built the respective 1000 colour-magnitude diagrams with the aim of considering the variation in the stellar

<sup>1</sup> <http://www.GEMINI.edu>

<sup>2</sup> Program kindly provided by P.B. Stetson

<sup>3</sup> We retrieved  $E(B - V)$  values from <https://irsa.ipac.caltech.edu/>

<sup>4</sup> <https://stev.oapd.inaf.it/cgi-bin/cmd>

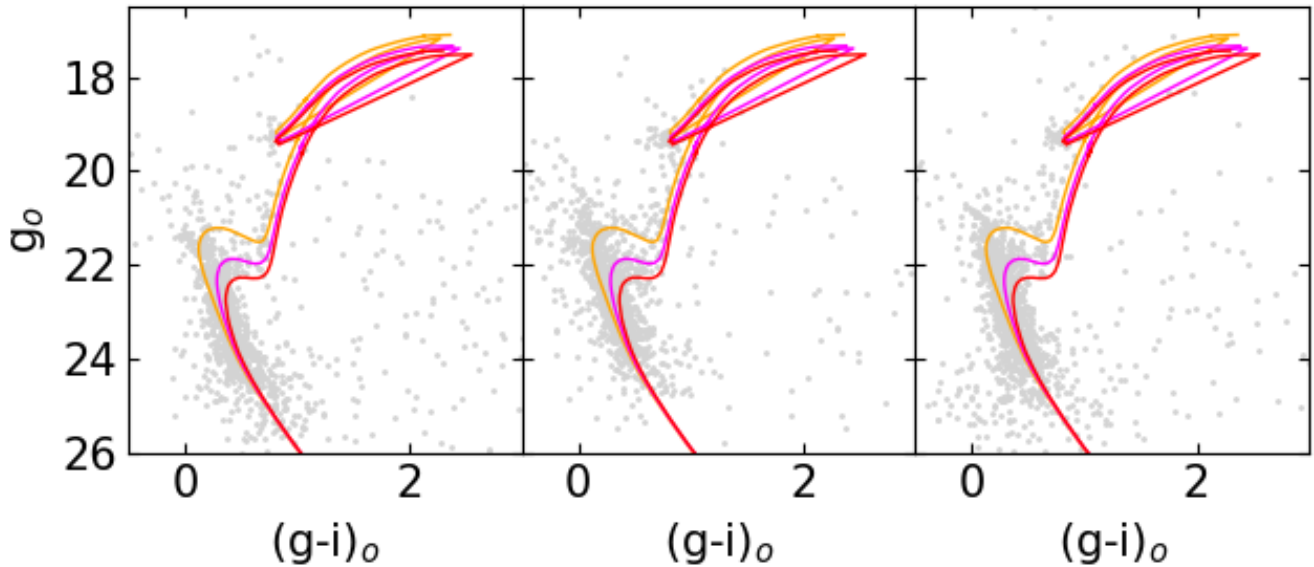


**Figure 2.** Colour-magnitude diagrams of the observed fields centred on STEP0004 (left), STEP0012 (middle), and YMCA0012 (right). Theoretical isochrones from Bressan et al. (2012) of 4, 7 and 10 Gyr for  $[\text{Fe}/\text{H}] = -0.7$  dex are superimposed with orange, magenta and red curves, respectively. We adopted  $E(B - V) = 0.10$  mag and  $(m - M)_o = 18.49$  mag (see text for details).

density and in the magnitude and colour distributions across the objects’ neighbouring regions. The procedure to select stars to subtract from the object colour-magnitude diagram follows the precepts outlined by Piatti & Bica (2012). We applied it using one star field colour-magnitude diagram at a time to be compared with the object colour-magnitude diagram. It consists in defining boxes centred on the magnitude and colour of each star of the star field colour-magnitude diagram; then to superimpose them on the object colour-magnitude diagram, and finally to choose one star per box to subtract. In order to guarantee that at least one star is found within the box boundary, we considered boxes with size of  $(\Delta g, \Delta(g - i)) = (1.00 \text{ mag}, 0.40 \text{ mag})$ . In the case that more than one star is located inside a box, the closest one to its centre is subtracted. During the choice of the subtracted stars we took into account their magnitude and colour errors by allowing them to have a thousand different values of magnitude and colour within an interval of  $\pm 1\sigma$ , where  $\sigma$  represents the errors in their magnitude and colour, respectively. We also imposed the condition that the spatial positions of the subtracted stars were chosen randomly. In practice, for each field star we randomly selected a position in the object’s circle and searched for a star to subtract within a box of  $0.1'$  side. We iterated this loop up to 1000 times, if no star was found in the selected spatial box.

The outcome of the cleaning procedure is an object colour-magnitude diagram that likely contains only stars that represent the intrinsic features of that region. From the 1000 different cleaned object colour-magnitude diagrams, we defined a probability  $P$  (%) of being intrinsic magnitudes and colours as the ratio  $N/10$ , where  $N$  (between 0 and 1000) is the number of times a star was found among the 1000 different cleaned colour-magnitude diagrams. Figure 3 shows the resulting cleaned colour-magnitude diagrams for the three studied objects. They include with large filled

circles all the stars measured within the objects’ radii and coloured according to their respective  $P$  value.

### 3.2 Detection of stellar overdensities

Instead of cleaning the object colour-magnitude diagram, which implies assuming the existence of an intrinsic stellar overdensity, we performed alternatively a different approach consisting in detecting spatial clustering in the studied stellar fields. We used the HDBSCAN (Hierarchical Density-Based Spatial Clustering of Applications with Noise, Campello et al. 2013) Gaussian mixture model technique (Hunt & Reffert 2021) to search for spatial stellar overdensities in the  $(x, y)$  coordinates plane. The `min_cluster_size` parameter was varied between 2 and 15 dex in steps of 1 dex, and from the output we built the spatial stellar distribution plots as illustrated in Fig. 4 (top panels). We coloured points according to the `clusterer.labels_` parameter, which labels the different groups of stars identified by HDBSCAN.

The number of groups and the stars included in them can vary with the `min_cluster_size` parameter. Therefore, we visually inspected Figure 4 looking for the optimum `min_cluster_size` value towards which the `clusterer.labels_` values remain constant and with similar star distributions. Each `clusterer.labels_` value corresponds to a particular group of stars in Figure 4. HDBSCAN provides also the membership probability of each star to the corresponding group, all of them with membership probabilities higher than 90%. For comparison purposes, we built colour-magnitude diagrams for the group of stars identified at the centre of each observed field, which is in excellent agreement with the positions of the objects identified by Gatto et al. (2020), and three additional detected overdensities with similar dimensions like those of the studied objects.

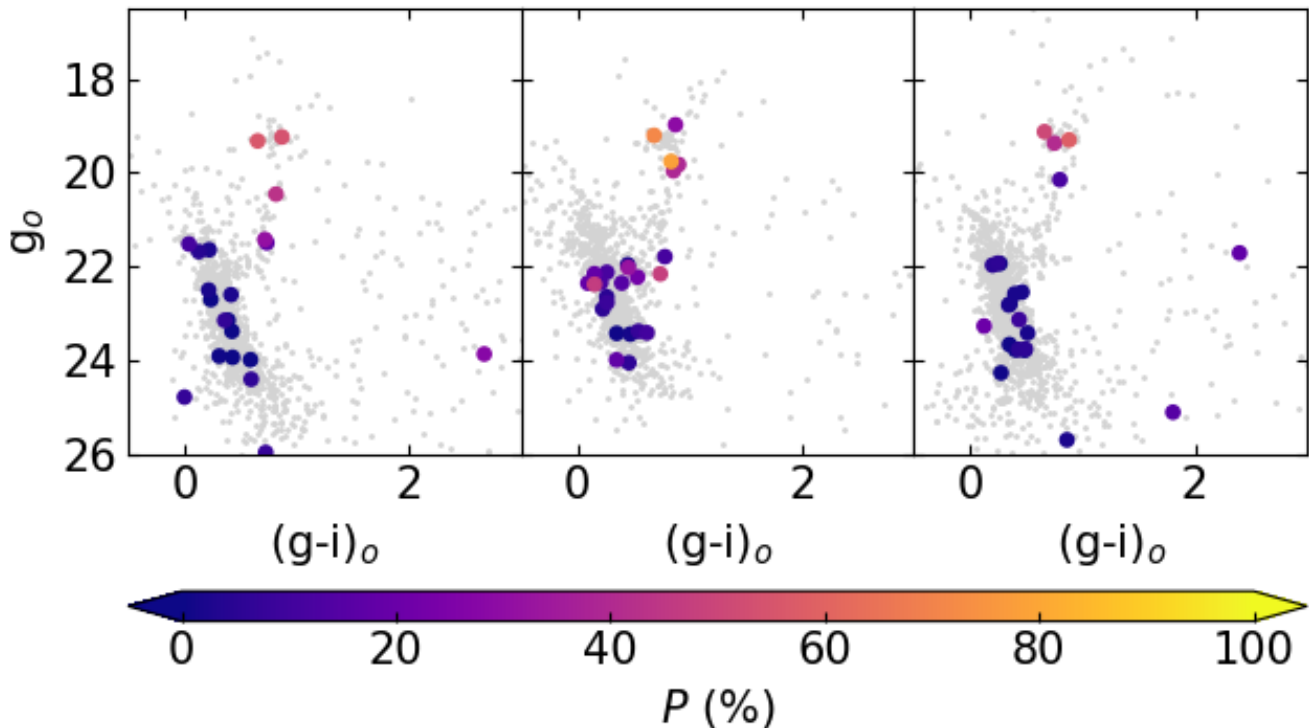


**Figure 3.** Cleaned colour-magnitude diagrams built from the present GEMINI data of STEP0004 (left), STEP0012 (middle), and YMCA0012 (right). The colour bar represents (in %) how much the magnitude and colour of a star differ from the magnitude and colour distribution of the projected surrounding LMC star field population. The grey points represent all the measured stars.

The chosen overdensities are encircled in the top panels of Figure 4, while their colour-magnitude diagrams are shown in the bottom panels, respectively, drawn with the corresponding colours.

#### 4 DISCUSSION

We started examining the schematic finding charts built by Gatto et al. (2020) for all their studied star clusters. They distinguished stars with cluster membership probability smaller than 25%, equals to 50%, and higher than 75%, respectively. As can be seen (their Figure B1), the analysed area would seem to be nearly nine times larger than the clusters' ones. Curiously, stars with cluster membership probabilities higher than 75% are distributed throughout the entire analysed region, which implies that stars with magnitudes and colours similar to those of clusters' members are also spread outside the clusters' areas. This behaviour could mean either that: 1) the field star cleaning colour-magnitude diagram procedure used was not able to robustly clean the analysed regions around the clusters' areas, which weakens the reliability of the assigned membership probabilities; or 2) stars with magnitudes and colours similar to those located in the clusters' areas already exist across the entire analysed regions, which would imply that the Gatto et al. (2020)'s candidates could be the result of variation (over-density) of the composite LMC star field population. Note that this effect is seen in all the studied clusters regardless their ages.

The LMC disc has an inclination of  $34^\circ$  and a position angle of the line of node of  $139.1^\circ$  (van der Marel & Kalliyayilil 2014). This means that the heliocentric distances of star clusters located in the LMC outer disc are different from that of the LMC geometrical centre. Particularly, the studied objects located at projected distances of  $\sim 5^\circ$  and position angles of  $\sim 230^\circ$  (see Figure 1) could be on average nearly 5 kpc behind the LMC centre (eq. (1) of Santos et al. (2020)), which implies a difference in their distance moduli with respect to the mean value for the LMC of  $\sim 0.20$ - $0.25$  mag. If we used the theoretical isochrones of Bressan et al. (2012) for the  $g$  versus  $g - i$  colour-magnitude diagram, we would find that a  $0.20$ - $0.25$  mag shift in distance modulus translates into a difference of age  $\gtrsim 2$  Gyr, for ages in the gap age range. Gatto et al. (2020) adopted the mean LMC distance modulus when fitting theoretical isochrones for all the clusters, so that their derived ages for the presently studied objects could be underestimated. They derived ages of 8.9, 7.1 and 8.9 Gyr for STEP0004, STEP0012, and YMCA0012, respectively, so that by adding 2 Gyr these objects would fall nearly at the upper end or outside the LMC age gap.

Gatto et al. (2020) derived overall metallicities for the studied objects of  $[M/H] = -0.40$  dex. Combining this value with the estimated ages, the objects would seem to fall well outside the LMC age-metallicity relation, whose average value is  $\sim -0.75$  dex for the gap age range (Piatti 2021b, and references therein). A mean metallicity of  $[M/H] = -0.40$  dex is typical of LMC stellar populations younger than 2 Gyr, which are mostly confined to the inner LMC disc and bar (Piatti & Geisler 2013). Although neither the unexpected

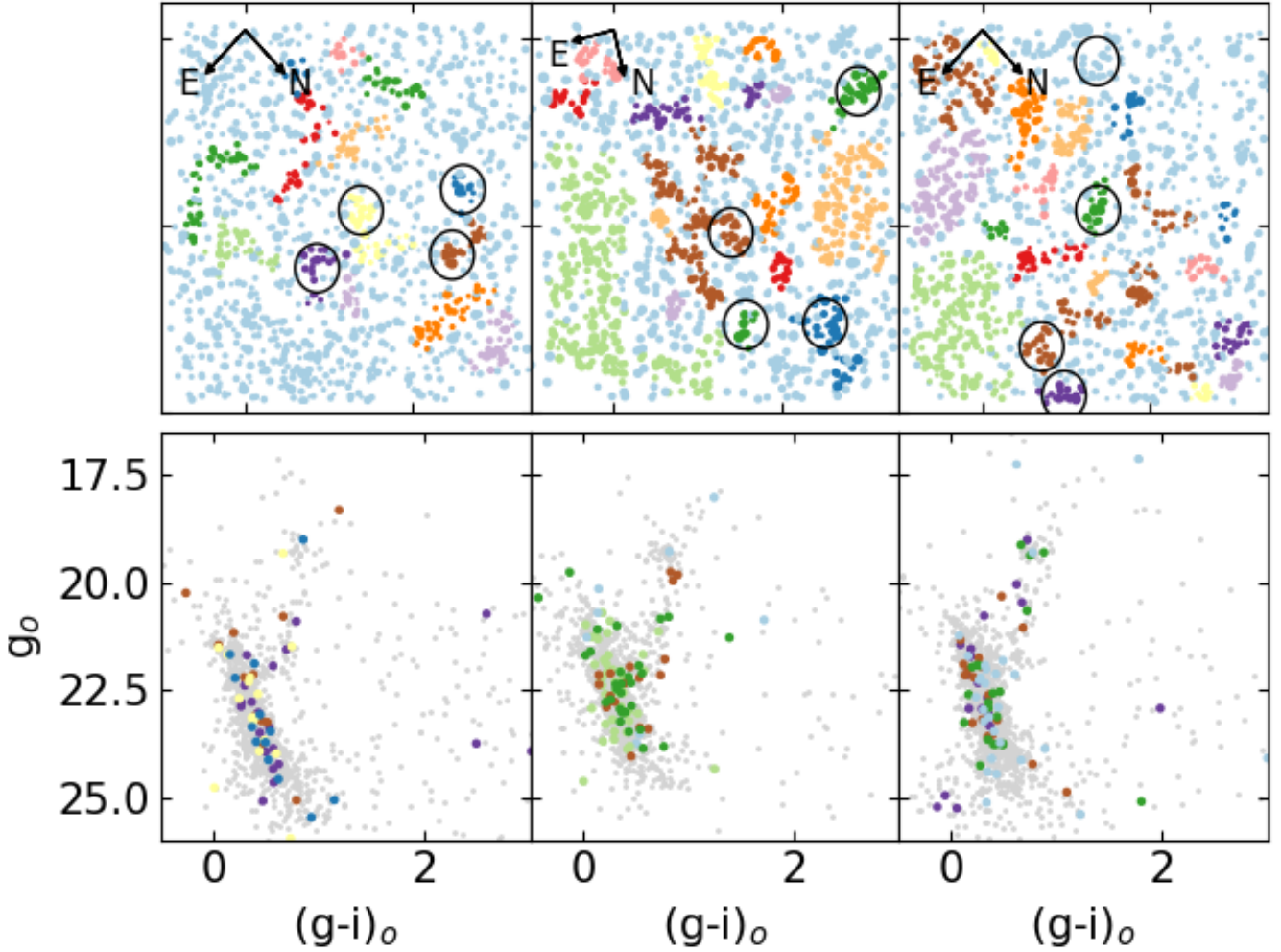


**Figure 4.** Spatial distribution of the measured stars from the present GEMINI data in the fields of STEP0004, STEP0012, and YMCA0012, from top left to top right panels, respectively, with the identified HDBSCAN stellar overdensities distinguished with different coloured symbols. The bottom panels show the colour-magnitude diagrams of the group of stars encircled with black circles in the top panels, respectively.

derived metallicities, nor the adopted mean distance modulus, nor the assigned membership probabilities are conclusive evidence against the physical nature of the studied objects as LMC age gap clusters, all of them considered together represent a volume of outcomes that discourage confidently concluding on the studied objects as real star clusters. They would rather seem to be fluctuations of the stellar density along the line-of-sight.

The procedure to assign probabilities  $P$  described in Section 3.1 has been tested and validated elsewhere (see, e.g., Piatti & Lucchini 2022; Piatti 2022b, and references therein). Particularly, we applied it to KMHK 1592, an LMC star cluster projected toward a relatively crowded star field (see Figure 1). For that purpose, we used a set of data obtained with the GEMINI South telescope in combination with the GMOS-S instrument and the  $g$  and  $i$  filters, similarly as the present data sets, and clearly disentangled its sub-giant and red giant branches (see Piatti 2022a). As a matter of providing additional examples of the robustness of the cleaning procedure, we included in the Appendix the

analysis of a well known LMC star cluster, as well as the corresponding HDBSCAN results.

Figure 3 shows that the measured stars placed within the adopted radii of the studied objects are mostly main sequence stars with a probability higher than 90% ( $P < 10\%$ ) of having magnitudes and colours representative of the projected LMC star field populations, and a couple of red clump stars that can be either part of the surrounding field or a local enhancement. There is no cluster sequences composed of stars that represent the excess of stars over the mean field stellar density is still smaller. Because of the relatively large heliocentric distance of the LMC, its composite field star population, or a small portion of it, can appear distributed in the colour-magnitude diagram similarly to clusters' stars.

In order to probe that small LMC field star overdensities can mimic star cluster colour-magnitude diagrams, we

performed a blind search of stellar overdensities using the HDBSCAN engine. By entering HDBSCAN simply with the  $x$  and  $y$  coordinates of all the measured stars in a given observed field, HDBSCAN identified tens of stellar overdensities of different size, shape and number of stars. Fortunately, HDBSCAN also identified the stellar overdensities called by Gatto et al. (2020) STEP0004, STEP0012, and YMCA0012, located at the centre of their respective observed fields. Top panels of Figure 4 illustrate these findings. Using the stars belonging to the identified stellar overdensities, we built the colour-magnitude diagrams of STEP0004, STEP0012, and YMCA0012 and those of three randomly selected stellar overdensities per observed field with sizes similar to the studied objects. As can be seen in the bottom panels of Figure 4, the colour-magnitude diagrams resemble those of star clusters with the unavoidable presence of some outliers. The randomly chosen stellar overdensities have not been catalogued as star cluster candidates. Nevertheless, we applied to their colour-magnitude diagrams the cleaning procedure of Section 3.1, and found that all their stars have  $P < 10\%$ .

Piatti (2021a) applied the procedure to remove the contamination caused by field stars in the colour-magnitude diagrams to all the LMC age gap cluster candidates identified by Gatto et al. (2020), using their same data sets and that of SMASH DR2 (Nidever et al. 2021), to further confirm the ages of the new star cluster candidates, so to reinforce their discoveries. He concluded that the objects would be LMC star field density fluctuations rather than age gap star clusters, despite neither Gatto et al. (2020) nor SMASH surveys have the ability to disentangle the existence of LMC age gap star clusters. He pointed to the need of further deeper observations of these star cluster candidates with the aim of providing a definite assessment on their physical realities. Indeed, the present GEMINI data sets would seem to discard any strong evidence of STEP0004, STEP0012, and YMCA0012 being real star clusters. Since Piatti (2021a) and present results are in agreement, we concluded that the remaining LMC age gap cluster candidates with no deeper observations could also be a group of stars with similar properties like those of the studied objects. We note that there are other characteristics that a group of stars must comply with in order to be confirmed as a genuine open cluster, such as a stellar number density profile, a cluster mass function, a mean metallicity, a relation between cluster mass and cluster radius, among others (Piatti et al. 2023).

Additionally, based only on the similar spatial distribution of the three observed fields and that of the remaining Gatto et al. (2020)'s candidates (see figure 1), we found that the present results for the studied objects could be extended to nearly 50% of the whole Gatto et al. (2020)'s candidate sample. In order to obtain such a completeness probability, we used eq. (1) of Piatti (2017), which combines the ratio of the number of observed fields to the total number of LMC age gap cluster candidates and a measure of the similarity between their spatial distributions, respectively. Thus, the better an LMC area is covered by the analysed fields, the higher the similarity of their respective spatial distributions. To obtain a measure of the spatial similarity we employed the *kde.test* statistical function provided by the *ks* package

(version 1.10.4)<sup>5</sup>. We assumed the null hypothesis is true, of observing a result at least as extreme as the value of the test statistic (Feigelson & Babu 2012). Here the null hypothesis is that  $(x, y)$  coordinate samples for studied objects and for the whole object sample come from the same underlying distribution. We obtained a similarity value of 0.95. Therefore, it would not seem to be obvious that a substantial number of LMC age gap cluster candidates are real star clusters.

Indeed, by looking at Figure 1 of Gatto et al. (2020), the candidates come from a limited number of tiles analysed, which in turn represent a minor percentage of the whole survey area coverage. Their concentration in a relatively small region could infer the occurrence of a bursting LMC age gap formation episode, which contrast with the spatial distribution of the three known LMC age gap clusters, scattered across the outer LMC disc on the other side of the galaxy (see Figure 1).

With accurate heliocentric distances, proper motions and radial velocities, it could be possible to trace the star cluster orbits backward in time for a time interval equals to their ages, in order to recover their birthplaces. (Piatti & Lucchini 2022) performed such an analysis to conclude that the recently discovered stellar system YMCA-1 is a moderately old SMC star cluster that could be stripped by the LMC during any of the close interactions between both galaxies, and now is seen to the East from the LMC centre. By starting with the modelling of the orbital motions of ESO 121-SC03, KMHK 1592 and KMHK 1762 –the three known LMC age gap clusters– we could infer whether they have been subject of tidal stripping, so that we presently observe them in the outer LMC disc. Indeed, Vasiliev (2024) found that the first close passage of the LMC by the Milky Way could have happened between  $\sim 5$ -10 Gyr ago, just along the LMC age gap. This is a promising scenario which deserves further attention by the next generation of numerical models of LMC cluster orbits, in order to explain the lack of more LMC clusters with ages between  $\sim 4$  and 11 Gyr. Because of the apparent fruitless efforts in the search for LMC age gap clusters from the present results, it would seem suggestive to focus further analysis on the improvement of the LMC cluster formation history that involves galaxy interactions.

## 5 CONCLUSIONS

The LMC cluster age gap is a phenomenon that still remains not understood in the context of our knowledge of the LMC star cluster formation and evolution. It is related to the lack of star clusters with ages between  $\sim 4$  and 11 Gyr as numerous as those expected. Recently, Gatto et al. (2020) discovered a number of LMC age gap cluster candidates that matches those expectations. Because of the need of deeper colour-magnitude diagrams to reliably estimate their ages, we carried out GEMINI@GMOS observations of three of these candidates, namely: STEP0004, STEP0012 and YMCA0012. The outcomes of our data analysis can be summarized as follows:

<sup>5</sup> <http://www.mvstat.net/tduong>.

- The inspection of their colour-magnitude diagrams, once they were cleaned of the presence of field stars, would suggest that the stars which represent an excess over the mean field star spatial density distribution have in general probabilities of being cluster members smaller than 10%.

- Across the observed fields we identified many other stellar overdensities distributed around the star cluster candidates. They have not been catalogued as star cluster candidates. Moreover, when we inspected their colour-magnitude diagrams decontaminated from field stars, we found in general stars with probabilities of being part of physical star groups smaller than 10%, as expected.

- Even in the case of assuming the existence of real star clusters, the procedure to estimate their astrophysical parameters employed by [Gatto et al. \(2020\)](#) could mislead the results. For instance, they adopted the mean LMC heliocentric distance as the clusters' distance, which could imply to estimate ages younger than  $\sim 2$  Gyr. The derived metal content for these star cluster candidates put them at the same time among the population of LMC clusters younger than  $\sim 2$  Gyr

- Because of the similar spatial distribution in the LMC of the three studied objects and that of the remaining age gap cluster candidates of [Gatto et al. \(2020\)](#), the present results on the presence of field star density variations instead of the existence of real star clusters, could be extended to nearly 50% of the whole sample.

- The lack of detection of more LMC age gap clusters point to the need of exploring different cluster formation and evolution models that include the gravitational effects from the interaction between the involved galaxies. Particularly, we speculate with the possibility that a number of LMC age gap clusters could have been ejected because a close encounter between the LMC and the Milky Way, that could have happened according to recent theoretical simulations at that space of time.

## ACKNOWLEDGEMENTS

We thank the referee for the thorough reading of the manuscript and timely suggestions to improve it.

Based on observations obtained at the international GEMINI Observatory, a program of NSF NOIRLab, which is managed by the Association of Universities for Research in Astronomy (AURA) under a cooperative agreement with the U.S. National Science Foundation on behalf of the GEMINI Observatory partnership: the U.S. National Science Foundation (United States), National Research Council (Canada), Agencia Nacional de Investigación y Desarrollo (Chile), Ministerio de Ciencia, Tecnología e Innovación (Argentina), Ministério da Ciência, Tecnologia, Inovações e Comunicações (Brazil), and Korea Astronomy and Space Science Institute (Republic of Korea).

## 6 DATA AVAILABILITY

Data used in this work are available upon request to the author.

## REFERENCES

- Babusiaux C., et al., 2023, *A&A*, **674**, A32  
 Bekki K., Couch W. J., Beasley M. A., Forbes D. A., Chiba M., Da Costa G. S., 2004, *ApJ*, **610**, L93  
 Besla G., Kallivayalil N., Hernquist L., Robertson B., Cox T. J., van der Marel R. P., Alcock C., 2007, *ApJ*, **668**, 949  
 Bica E., Bonatto C., Dutra C. M., Santos J. F. C., 2008, *MNRAS*, **389**, 678  
 Bressan A., Marigo P., Girardi L., Salasnich B., Dal Cero C., Rubele S., Nanni A., 2012, *MNRAS*, **427**, 127  
 Campello R. J. G. B., Moulavi D., Sander J., 2013, in Pei J., Tseng V. S., Cao L., Motoda H., Hu G., eds, *Pacific-Asia Conference on Knowledge Discovery and Data Mining*. Springer, Berlin, Heidelberg, 160-172  
 Carpintero D. D., Gómez F. A., Piatti A. E., 2013, *MNRAS*, **435**, L63  
 Choi Y., Olsen K. A. G., Besla G., van der Marel R. P., Zivick P., Kallivayalil N., Nidever D. L., 2022, *ApJ*, **927**, 153  
 Cioni M.-R. L., et al., 2011, *A&A*, **527**, A116  
 Da Costa G. S., 1991, in Haynes R., Milne D., eds, *IAU Symposium Vol. 148, The Magellanic Clouds*. p. 183  
 Da Costa G. S., Hatzidimitriou D., 1998, *AJ*, **115**, 1934  
 Feigelson E. D., Babu G. J., 2012, *Modern Statistical Methods for Astronomy*  
 Gaia Collaboration et al., 2016, *A&A*, **595**, A1  
 Gatto M., et al., 2020, *MNRAS*, **499**, A114  
 Gatto M., et al., 2022, *A&A*, **664**, L12  
 Gatto M., et al., 2024, *A&A*, **690**, A164  
 Geisler D., Bica E., Dottori H., Claria J. J., Piatti A. E., Santos Jr. J. F. C., 1997, *AJ*, **114**, 1920  
 Harris J., Zaritsky D., 2009, *AJ*, **138**, 1243  
 Hunt E. L., Reffert S., 2021, *A&A*, **646**, A104  
 Jiménez-Arranz Ó., et al., 2023, *A&A*, **669**, A91  
 Massana P., et al., 2022, *MNRAS*, **513**, L40  
 Mateo M., Hodge P., Schommer R. A., 1986, *ApJ*, **311**, 113  
 Narloch W., et al., 2022, *A&A*, **666**, A80  
 Nidever D. L., et al., 2017, *AJ*, **154**, 199  
 Nidever D. L., et al., 2021, *AJ*, **161**, 74  
 Pagel B. E. J., Tautvaisiene G., 1998, *MNRAS*, **299**, 535  
 Piatti A. E., 2013, *MNRAS*, **430**, 2358  
 Piatti A. E., 2016, *MNRAS*,  
 Piatti A. E., 2017, *ApJ*, **834**, L14  
 Piatti A. E., 2021a, *AJ*, **161**, 199  
 Piatti A. E., 2021b, *A&A*, **647**, A47  
 Piatti A. E., 2022a, *MNRAS*, **511**, L72  
 Piatti A. E., 2022b, *MNRAS*, **514**, 4982  
 Piatti A. E., Bica E., 2012, *MNRAS*, **425**, 3085  
 Piatti A. E., Geisler D., 2013, *AJ*, **145**, 17  
 Piatti A. E., Lucchini S., 2022, *MNRAS*, **515**, 4005  
 Piatti A. E., Keller S. C., Mackey A. D., Da Costa G. S., 2014, *MNRAS*, **444**, 1425  
 Piatti A. E., Salinas R., Grebel E. K., 2019a, *MNRAS*, **482**, 980  
 Piatti A. E., Alfaro E. J., Cantat-Gaudin T., 2019b, *MNRAS*, **484**, L19  
 Piatti A. E., Illesca D. M. F., Massara A. A., Chiarpotti M., Roldán D., Morón M., Bazzoni F., 2023, *MNRAS*, **518**, 6216  
 Ripepi V., et al., 2014, *MNRAS*, **442**, 1897  
 Santos João F. C. J., et al., 2020, *MNRAS*, **498**, 205  
 Schmidt T., et al., 2022, *A&A*, **663**, A107

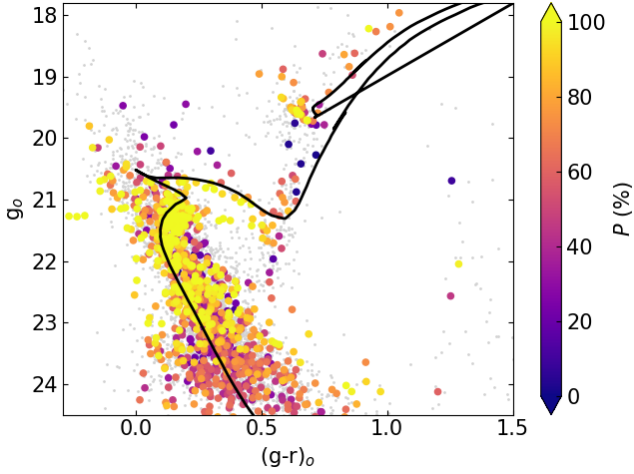


**Figure A1.** Cleaned colour-magnitude diagrams of stars measured in the field of SL 529 built from GEMINI data of Piatti (2013). The colour bar represents (in %) how much the magnitude and colour of a star differ from the magnitude and colour distribution of the projected surrounding LMC star field population. The grey points represent all the measured stars. A theoretical isochrones from Bressan et al. (2012) of 2.25 Gyr and  $[\text{Fe}/\text{H}] = -0.60$  dex is superimposed. We adopted  $E(B - V) = 0.04$  mag and  $(m - M)_o = 18.49$  mag.

Stetson P. B., Davis L. E., Crabtree D. R., 1990, in Jacoby G. H., ed., *Astronomical Society of the Pacific Conference Series Vol. 8, CCDs in astronomy*. pp 289–304  
 Vasiliev E., 2024, *MNRAS*, 527, 437  
 de Grijs R., Wicker J. E., Bono G., 2014, *AJ*, 147, 122  
 van der Marel R. P., Kallivayalil N., 2014, *ApJ*, 781, 121

## APPENDIX A: CMD ANALYSIS AND STELLAR OVERDENSITIES

With the aim of providing additional examples of the performance of the procedures applied in Sections 3.1 and 3.2, we used GEMINI@GMOS data obtained by Piatti (2013) for the LMC star cluster SL 529. In Figure A1 we show the CMD of the stars measured in the cluster’s field, similar to Figure 3. We superimposed the theoretical isochrone from Bressan et al. (2012) for the cluster’s age (2.25 Gyr) and metallicity ( $[\text{Fe}/\text{H}] = -0.60$  dex), and adopting the cluster’s reddening ( $E(B - V) = 0.04$  mag) and distance modulus (18.49 mag), for comparison purposes. In Figure A2 we show for SL 529 a figure similar to Figure 4, built from the outcomes of the HDBSCAN method.

This paper has been typeset from a  $\text{T}_{\text{E}}\text{X}/\text{L}^{\text{A}}\text{T}_{\text{E}}\text{X}$  file prepared by the author.

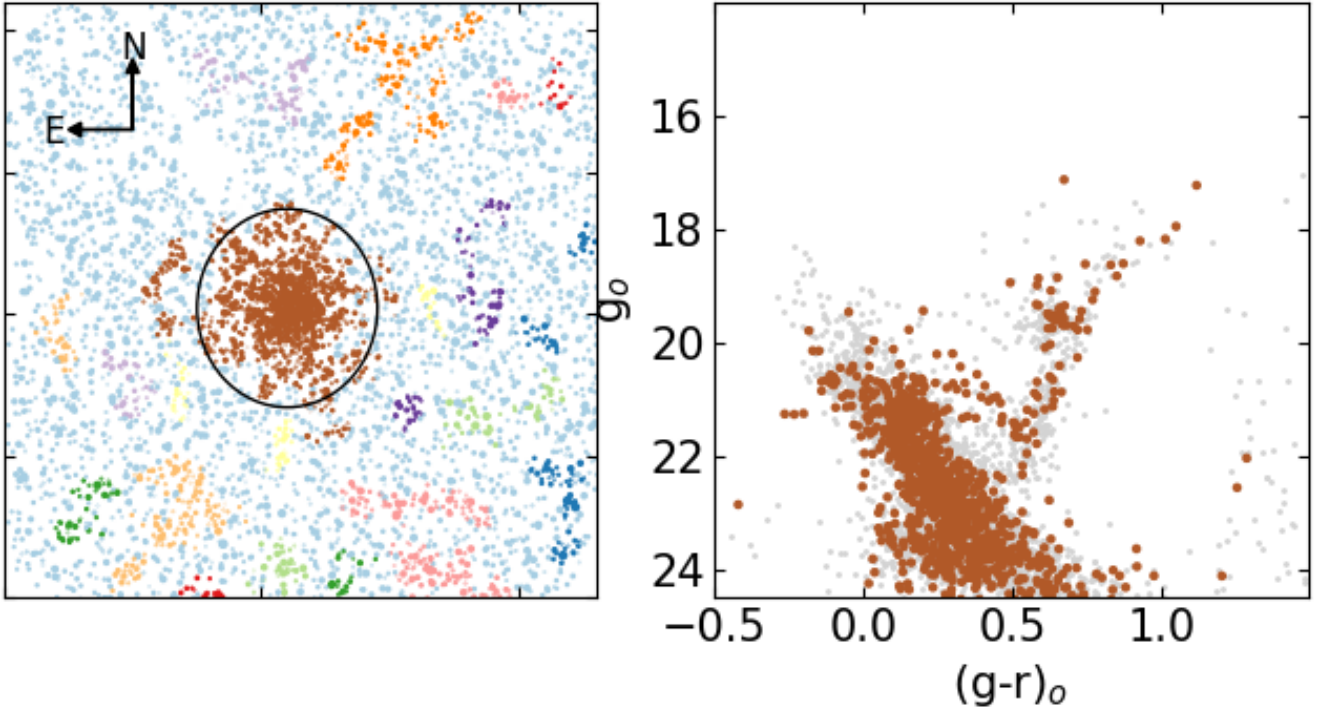


**Figure A2.** Spatial distribution of the measured stars in the field of SL 529 with the identified HDBSCAN stellar overdensities distinguished with different coloured symbols. The right panel shows the colour-magnitude diagram of the group of stars encircled with black circle in the left panel.